OPTICAL REVIEW Vol. 20, No. 5 (2013) 378–384

Liquid Crystal Retarder Spectral Retardance Characterization Based on a Cauchy Dispersion Relation and a Voltage Transfer Function

Asticio VARGAS[1,2], Ramiro DONOSO[1,2], Manuel RAMÍREZ[1,2], José CARRIÓN[3], María del Mar SÁNCHEZ-LÓPEZ[4], and Ignacio MORENO[3]

[1]*Departamento de Ciencias Físicas, Universidad de La Frontera, Temuco, Chile*
[2]*Center for Optics and Photonics, Universidad de Concepción, Casilla 4016, Concepción, Chile*
[3]*Departamento de Ciencia de Materiales, Óptica y Tecnología Electrónica, Universidad Miguel Hernández, 03202 Elche, Spain*
[4]*Instituto de Bioingeniería, Universidad Miguel Hernández, 03202 Elche, Spain*

(Received May 29, 2013; revised June 19, 2013; Accepted June 25, 2013)

We present a methodology for the spectral characterization of the optical modulation properties of a liquid crystal retarder (LCR). The method includes its complete description with a single Cauchy dispersion relation and a single voltage transfer function. As a result, an accurate description of the LCR retardance is achieved, both versus applied voltage and versus wavelength, with very few parameters. Finally, an imaging polarimetric system has also been developed to characterize the spatial variations in the device.

Keywords: liquid crystal retarder, Cauchy dispersion formula, spectral retardance

1. Introduction

Liquid crystal retarders (LCR) are very useful devices for polarization control. They act as low order wave-plates. Upon application of a low voltage through the transparent electrodes, the LC director is forced to tilt, and the retardance can be continuously varied. Thus, they act as reconfigurable wave-plates, where the retardance can be adjusted to a desired value, with uses in heterodyne interferometers or polarimetric sensor systems. Such LCR devices are commercially available from a number of companies, like for instance Meadowlark Optics, Thorlabs Inc., or ArcOptix, with different prices and characteristics like effective area or modulation range.[1)] Manufacturers usually only provide some limited information. Therefore, developing simple methods to obtain accurate retardance measurements, both versus wavelength and versus applied voltage, is interesting to achieve a good device operation.

Several methods have been proposed in the literature to measure the retardance of wave plates with fixed retardance.[2–5)] The most precise ones are based on heterodyne measurements. Because they require illumination with a monochromatic laser beam, the retardance is measured only for this specific wavelength. In addition, they usually provide a relative measurement of the retardance, a modulo 2π value. The determination of the order in multiple-order wave plates require additional sequential measurements.[5)]

However, the retardance of simple single layer wave-plates typically presents an important dispersion, which usually varies inversely with the operating wavelength.[6)] Therefore it is very desirable to develop simple but still accurate methods for the broadband range retardance characterization in such devices. In general, the application of polarimetric techniques permits to retrieve this complete information.[7)] However, LCRs can be considered simply as linear waveplates with fixed orientation of the principal axis and variable retardance. Under this assumption, an accurate measurement of the retardance can be performed simply by intensity measurements when placing the wave-plate in between linear parallel or crossed polarizers, oriented at $\pm 45^\circ$ with respect to the principal axis. Such simple system, when illuminated with polychromatic light with continuous broadband spectrum, presents a spectral transmission with sinusoidal oscillations.[8,9)] Note that the continuous variation versus wavelength makes it possible to derive the retardance absolute value.

Retardance measurements of LCR versus voltage have been traditionally performed with the same optical configuration as described above. There, when monochromatic light illuminates the polarizer–LCR–analyzer system, sinusoidal oscillations are observed in the transmission versus applied voltage.[10,11)] Determination of the LC refractive indices and retardance by means of spectral measurements were reported already in the early stages of LC technology.[12)] More recently, spectral measurements have been used to determine parameters like the cell gap or the twist angle, in commercial twisted nematic LC devices.[13–16)]

In this work we apply such a simple spectral technique to measure the LCR retardance (ϕ), both as a function of wavelength (λ) and applied voltage (V). Our goal is to achieve a simple, but complete description of the retardance properties in the characterized wavelength range. For that purpose, a simple Cauchy dispersion relation is adopted to describe the spectral retardance and fit the experimental data. The fitting process is performed without applied voltage, so the device presents its maximum retardance, and the determination of the Cauchy constants is more accurate. Then we demonstrate that the Cauchy dispersion relation must be fulfilled also when a voltage is applied, but with the fitting constants modulated by a voltage transfer function. As a result, a full characterization of the device is retrieved with only two Cauchy constant parameters and a

single function that accounts for the voltage effect. The LCR spectral transmission can be predicted for any value of the applied voltage, and the transmission for a monochromatic beam within the selected wavelength range can be predicted as well.

The paper is organized as follows. In Sect. 2, the method for the spectral retardance determination is presented, including the Cauchy dispersion relation and the voltage transfer function are described. Section 3 presents the experimental setup and results. In Sect. 4 we include a simple polarimetric imaging system that provides the same type of measurements and displays a non-negligible spatial variation in the device retardance. Finally, Sect. 5 contains the conclusions of our work.

2. Method for the Spectral Retardance Measurement

Retardance measurements are usually performed with the classical system described above, where the retarder is inserted in between two linear polarizers which are oriented at 45° with respect to the neutral axes.[6] The normalized transmission is given by

$$i_{\text{parallel}} = \cos^2\left(\frac{\phi}{2}\right), \quad i_{\text{crossed}} = \sin^2\left(\frac{\phi}{2}\right), \tag{1}$$

for parallel and crossed polarizers, respectively. If the retarder is made of a single layer of anisotropic material (as it is the case for a LCR), the retardance reads as

$$\phi = \frac{2\pi d}{\lambda}\Delta n, \tag{2}$$

where λ is the wavelength, d is the physical thickness of the birefringent material layer (in this case the liquid crystal), and $\Delta n = n_e - n_o$ is the material birefringence, being n_o and n_e the ordinary and extraordinary refractive indices, respectively. Note that ϕ depends inversely on the wavelength. Therefore, according to Eq. (1), the light transmitted by this system will present an oscillatory transmission curve as a function of λ. Since the refractive indices also present dispersion, Δn will also contribute to the overall wavelength dependence.

2.1 *Cauchy approximation for the spectral dependence*

In general, the LC birefringence decreases as the wavelength increases in the visible region, and it remains approximately constant in the IR region, except for the resonance in the vicinity of the molecular vibrational bands.[6] A good approximation of the refractive index dispersion far from the absorption resonance is given by the Cauchy–type relation.[12,17] Using the first two terms in this approximation, both ordinary and extraordinary indices can be fitted to

$$n_{o/e} = a_{o/e} + \frac{b_{o/e}}{\lambda^2}, \tag{3}$$

where $a_{o/e}$ and $b_{o/e}$ are two constant parameters for each refractive index. Higher order terms can be incorporated, thus leading to the so-called extended Cauchy approximation. However, our results show that for the selected wavelength range (from 400 to 700 nm) it is enough to keep this simple approximation for our device. The determination of the liquid crystal refractive indices dispersion were reported by measuring the transmitted spectrum and fitting the Fabry-Perot interferences.[12] However, modern LCR devices incorporate anti-reflecting coating that minimize these effects, and much more advanced techniques, such as spectroscopic ellipsometry, would be required to characterize the refractive indices.[18] On the contrary, the retardance can be easily measured since it will present spectral variations.

Note that, if the Cauchy dispersion relation is adopted for the refractive indices, so does the birefringence Δn and, by applying Eq. (2), the retardance can be written as

$$\phi_0(\lambda) = \frac{A_0}{\lambda} + \frac{B_0}{\lambda^3}, \tag{4}$$

where A_0 and B_0 are constant parameters given by

$$A_0 = 2\pi(a_e - a_o)d, \quad B_0 = 2\pi(b_e - b_o)d. \tag{5}$$

Additional terms of the Cauchy approximation could be included, leading to additional terms in Eq. (4) proportional to λ^{-5}, λ^{-7}, ... However, for our device, and for the selected spectral range, fitting results are not improved significantly with these additional terms. Therefore, for simplicity, we adopt the relation in Eq. (4) to describe the experimental data.

2.2 *Voltage transfer function*

In these previous equations, subscripts "0" indicate that these values correspond to the LCR device in the absence of driving voltage. When a voltage (V) is applied, it results in a LC director molecular tilt, $\theta(V)$, that changes the effective extraordinary refractive index $n_{ef}(\theta)$, which is then given by

$$\frac{1}{n_{ef}^2(\theta)} = \frac{\sin^2(\theta)}{n_o^2} + \frac{\cos^2(\theta)}{n_e^2}. \tag{6}$$

The effective birefringence is voltage dependent, namely $\Delta n_{ef}(V) = n_{ef}(V) - n_o$; it is maximum without voltage, and diminishes as the LC director gets tilted.

We define a birefringence voltage transfer function that takes into account this reduction as

$$g(\theta(V)) \equiv \frac{n_{ef}(\theta(V)) - n_o}{n_e - n_o}. \tag{7}$$

Note that this normalization function ranges from 1 to 0 as the effective extraordinary index changes from n_e to n_o. Figure 1 shows the function $g(\theta)$ versus the tilt angle θ for a liquid crystal with some typical values as $n_o = 1.6$ and $n_e = 1.65$, 1.7, 1.8, and 1.9, respectively (birefringences $\Delta n = 0.05$, 0.1, 0.2, and 0.3 respectively). The function $g(\theta)$ monotonically decreases with the tilt angle, almost independently of the birefringence. Thus, $g(\theta)$ can be considered close to be a universal relation for practical values.[19]

The effective voltage and wavelength dependent retardance is given by

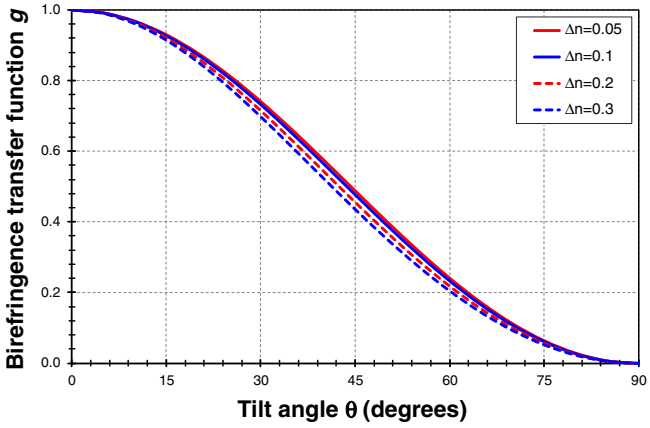

Fig. 1. (Color online) Birefringence transfer function $g(\theta)$ as a function of the tilt angle θ for a liquid crystal with $n_o = 1.6$ and $n_e = 1.65$, 1.7, 1.8, and 1.9, respectively (birefringences $\Delta n = 0.05$, 0.1, 0.2, and 0.3).

$$\phi_V(\lambda) = \frac{2\pi d}{\lambda} \Delta n_{ef}(\theta(V), \lambda), \tag{8}$$

which, from Eq. (7), can be written as

$$\phi_V(\lambda) = g(V)\phi_0(\lambda). \tag{9}$$

Therefore, if the off state LCR retardance $\phi_0(\lambda)$ follows a Cauchy dispersion relation [Eq. (4)], the voltage dependant retardance $\phi_V(\lambda)$ also must follow such type of relation, now given by:

$$\phi_V(\lambda) = \frac{g(V)A_0}{\lambda} + \frac{g(V)B_0}{\lambda^3}. \tag{10}$$

This relation indicate that the LC tilt reduces the retardance in the same proportion for all wavelengths.

Note that the above simple model implies that the molecular tilt is constant along the LC cell. Although this is not exact, it can be considered as a good approximation for homogeneously aligned devices, such as the LCR. In these cases, LC regions with different tilt contribute differently to the overall retardance, but the integration of the complete effect can be properly described with Eqs. (7)–(10), as demonstrated next. Therefore, within this approximation, the LCR voltage and wavelength behaviour can be fully characterized by just two constants parameters A_0 and B_0 and the birefringence voltage transfer function $g(V)$.

3. Experimental Setup and Results

Figure 2 shows a picture of the experimental setup. Broadband light from a tungsten lamp (Stellar-Net SL1, with 350–2200 nm wavelength range) is directed towards the polarizer–LCR–analyzer system by means of an optical fiber. The optical fiber output contains a lens that provides, approximately, a collimated beam. All elements are properly aligned so normal incidence can be assumed. The LCR device is from Meadowlark, model LRC-200 VIS. Some general aspects of LCR devices from this company can be found in Ref. 20. The device is placed in between two linear polarizers (Meadowlark Optics DPM-200-VIS). The transmitted light is captured with a second optical fiber and is directed to an spectrometer (Stellar-Net EPP2000HR-UV-VIS-NIR). The spectrometer can capture the light spectrum in the range from 200 to 1100 nm. However, we restrict our measurements to the visible range from 400 to 700 nm in order to assure the correct performance of the polarizers.

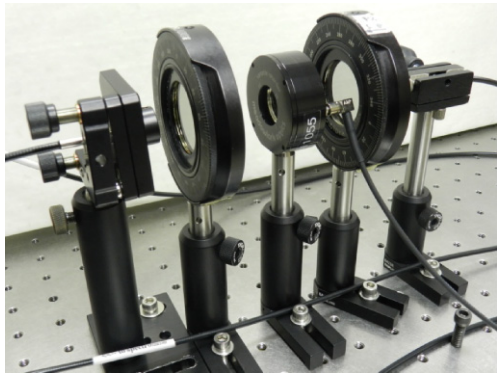

Fig. 2. (Color online) Photograph of the experimental setup.

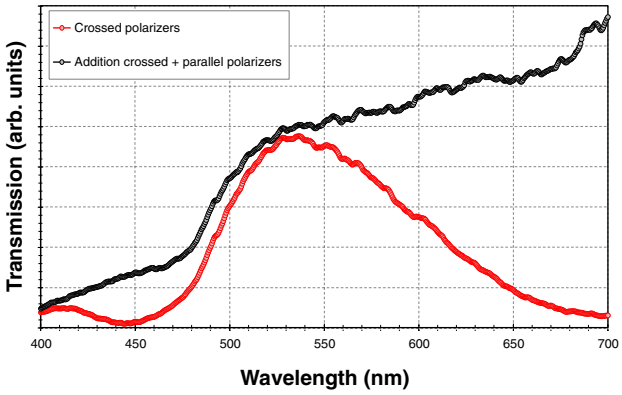

Fig. 3. (Color online) Experimental captured spectra when the input polarizer is oriented at 45° with respect to the LC director. Red curve corresponds to the measurement with the analyzer crossed to the input polarizer. Black curve corresponds to addition of the spectra with crossed and parallel polarizers.

Our first step was to locate the LCR neutral axes. For that purpose, the two polarizers were simultaneously rotated, keeping them always crossed, until maximum extinction was observed on the whole spectral range. Then, the input polarizer was rotated by 45°. The analyzer is oriented parallel or perpendicular to the input polarizer. Then, the oscillatory behavior predicted by Eq. (1) becomes present on the transmitted spectrum (red curve in Fig. 3). More than one complete oscillation occurs in the selected wavelength range, denoting a variation of more than 2π radians. A second curve is shown in Fig. 3, corresponding to the addition of the spectra captured for crossed and parallel polarizers. It therefore reproduces the total light emerging from the LCR device. This spectrum shows that the total energy decreases as the wavelength decreases. This is a consequence of using a tungsten lamp as the broadband light

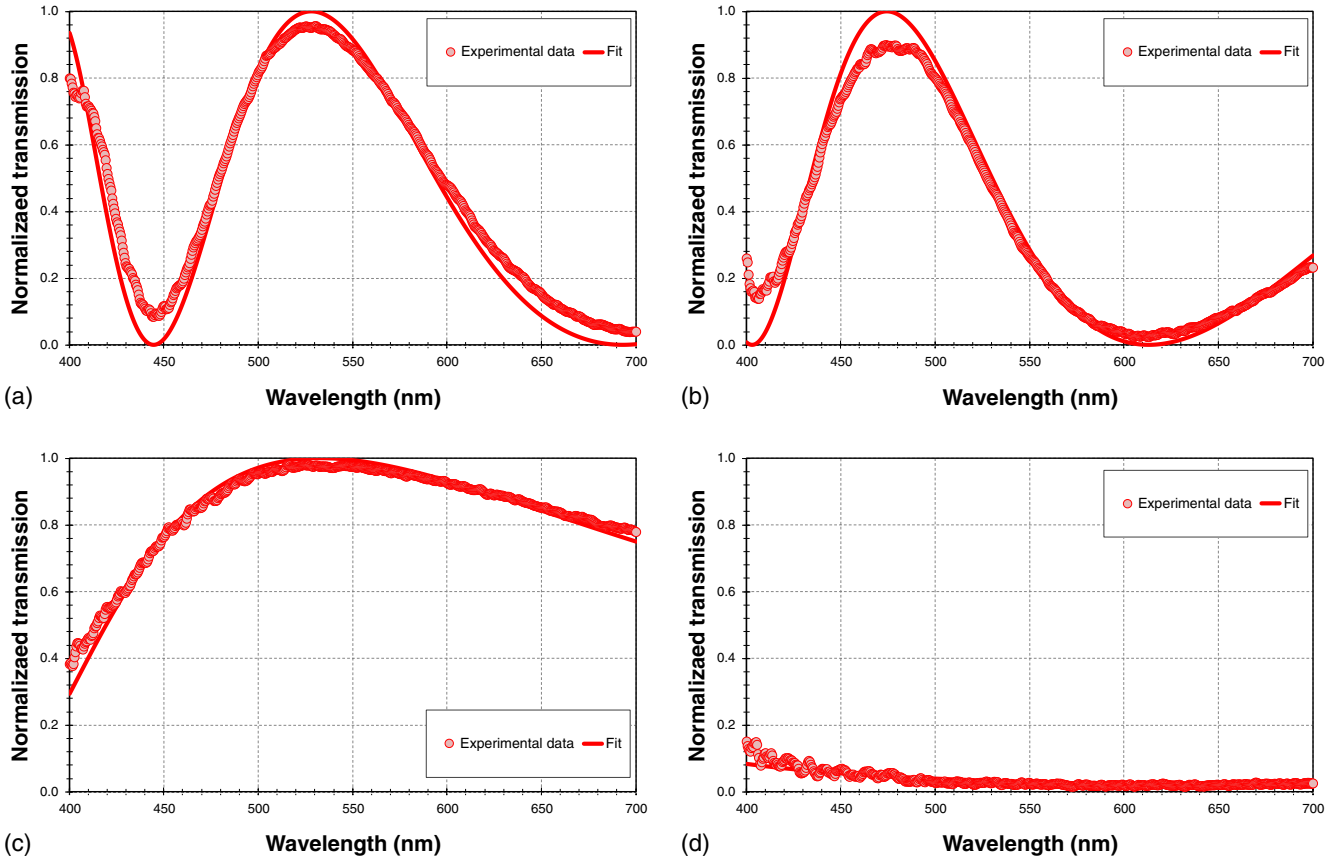

Fig. 4. (Color online) Experimental captured spectrum and best fit for crossed polarizers for different voltages: (a) $V = 0$, (b) $V = 2.0\,\mathrm{V}$, (c) $V = 3.5\,\mathrm{V}$, and (d) $V = 7.0\,\mathrm{V}$.

source. Results will be presented normalized to this curve. Note that the lamp provides low level of intensity at low wavelengths, and thus higher noise level is expected.

The fitting procedure involves comparing the spectral transmission with Eq. (1) with a spectral retardance given by Eq. (4). The two Cauchy constants A_0 and B_0 are employed to best fit the data in Fig. 3. Performing the Cauchy based fitting process with these data is advantageous since the LCR retardance is maximum. Data were normalized by dividing the spectrum for crossed polarizers by the addition of the spectra for crossed and parallel polarizers. The resulting normalized transmission is therefore in the range $[0, 1]$, which can be directly compared to the theoretical Eq. (1). These normalized data are presented in Fig. 4(a). Note that the experimental data do not reach values 0 and 1. We attribute this effect to the limited quality of the polarizers. However, the location of the maxima and minima denote the wavelengths for which the retardance is an integer multiple of π radians. Therefore, we force the calculation to obtain the maxima and minima at the same wavelengths as the experimental curve, and then minimize the difference between experimental and fitted curves. The results are in good agreement, as shown in Fig. 4. Figure 4(a) also shows the best fit, obtained for values $A_0 = 3493.35\,\mathrm{rad{\cdot}nm}$ and $B_0 = 4.13415 \times 10^8\,\mathrm{rad{\cdot}nm^3}$. Note that usually Cauchy fitting is performed with data in a reduced number of wavelengths. Here, since the spectrometer spectral resolution is 0.5 nm, 600 different wavelengths are employed.

Figures 4(b)–4(d) correspond to the spectrometer captures for driving voltages of 2.0, 3.5, and 7.0 V, respectively. In all cases, measurements are made in the same conditions with the light beam impinging exactly the same location on the LCR surface. Note that the oscillatory behaviour progressively reduces as the voltage increases. This indicates that, as expected, the LCR retardance diminishes. For each voltage, the retardance function $\phi_V(\lambda)$ in Eq. (10) is forced to adjust the experimental data by fitting the birefringence transfer function $g(V)$. The best fit is obtained with values $g(V = 2.0) = 0.838$, $g(V = 3.5) = 0.338$, and $g(V = 7.0) = 0.039$. Figure 5(a) shows the evolution with voltage of the birefringence transfer function $g(V)$, for voltage values in the range from 0 to 7 V. Figure 5(b) shows the corresponding results for the retardance $\phi_V(\lambda)$.

The results in Fig. 5 provides a complete spectral characterization of the LCR retardance. Therefore, the transmission of the polarizer–LCR–analyzer system can be predicted for any wavelength within the selected range. As an example, Fig. 5(a) indicates the retardance range for two specific wavelengths, $\lambda = 633\,\mathrm{nm}$ and $\lambda = 533\,\mathrm{nm}$. From this figure the maximum retardance for these two wavelengths is 2.28π radians and 2.96π radians respectively. As a verification, Fig. 6(a) shows the experimental transmission

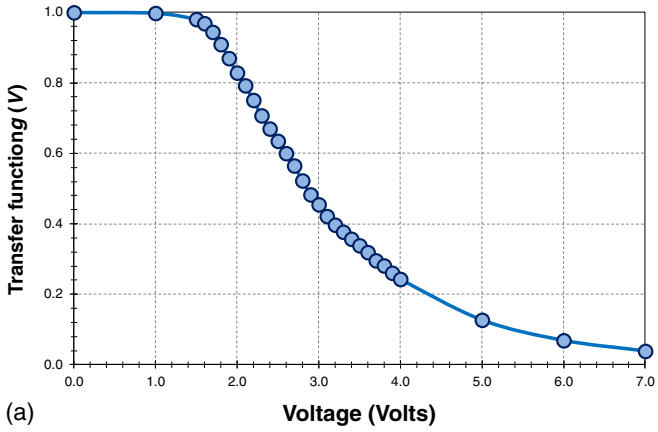

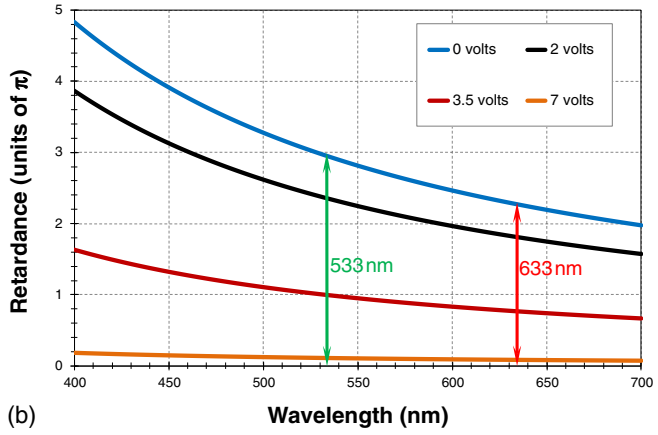

Fig. 5. (Color online) (a) Voltage transfer function $g(V)$. (b) Spectral retardance $\phi_V(\lambda)$ derived after Cauchy curve fitting for voltages $V = 0$, 2.5, 3.5, and 7 V.

versus applied voltage for two lasers with these wavelengths. In each case, the normalized transmission for the configuration with the input polarizer oriented at 45°, and with crossed analyzer is presented. Dots in Fig. 6(a) denote the experimental data, while the continuous curves denote the corresponding expected normalized transmission derived from the spectral phase shift calibration data in Fig. 5. As expected, the agreement is excellent.

4. Polarimetric Imaging to Detect Spatial Variations

The results in the two previous sections were obtained by carefully keeping the same area on the LCR illuminated. Although the Meadowlark LCR device has an effective circular aperture of 0.70 in, we placed an iris diaphragm just in front of it, in the central part of the device. Its aperture is approximately of 3 mm^2 (a radius of approximately 1 mm). The reason is that we noticed a non-negligible variation of the retardance at different points in the LCR. Achieving LCR with large uniform effective areas remains a fabrication challenge,[21] and often measurements must be done at multiple points.[22] Here we adopt instead an imaging characterization of the device.

Imaging polarimetry is an appropriate technique to perform such calibration, since it leads to complete

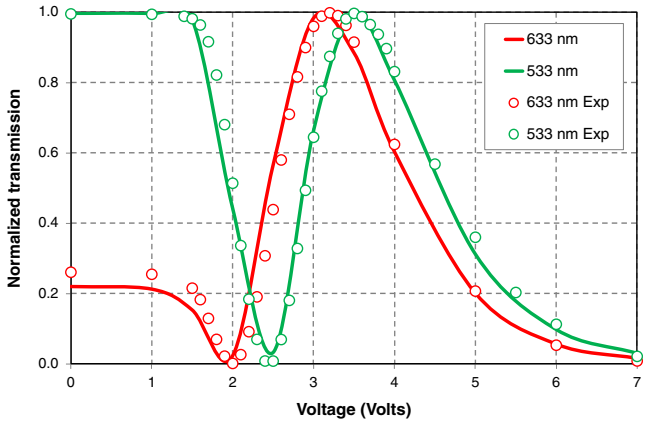

Fig. 6. (Color online) Experimental normalized transmission as a function of voltage for two different wavelengths (633 and 533 nm); the input polarizer is at 45°, and the analyzer is crossed.

measurements. However, measurements can be simplified again by assuming the device simply as a pure linear retarder, where the neutral axes remain fixed, but there is a spatial variation of the retardance. Application of the spectral method described previously would require the use of an hyperspectral camera.[23] Here, instead we use the classical calibration method with monochromatic illumination ($\lambda = 633$ nm) and employ a simple camera. We illuminated the LCR with a collimated beam with linear polarization oriented at 45°. The LCR surface was imaged onto a CCD camera (Basler piA1000-60gm) by means of a converging lens of focal length $f' = 12,5$ cm. An analyzer was placed just before the CCD, in order to select the image with parallel and crossed polarizers. From Eq. (1), the retardance for each voltage is calculated as

$$\phi_V = 2 \arctan\left(\sqrt{\frac{i_{\text{crossed}}}{i_{\text{parallel}}}}\right), \tag{11}$$

which is directly derived from Eq. (1). A phase unwrapping correction must be applied, since the previous equation only provides phase values in the range $[0, \pi]$ radians. We impose that the retardance must be continuous and monotonically increasing as the voltage decreases.

Figure 7(a) shows the captured images for various voltages when the polarizers are set parallel. For these voltage values, the phase shift is approximately π radians, and therefore a dark image should be obtained. We observe the dark area in the form of a diagonal line, but it is not homogeneous. Here the images were oversaturated for clarity. In order to obtain spatial retardance measurements, images were captured for parallel and crossed polarizers, avoiding saturation. Then, they were normalized pixel by pixel, with the same procedure as before and the retardance is derived at each point using Eq. (11). Figures 7(b) and 7(c) show the retardance curves versus voltage for two different points located in opposite regions of the LCR (indicated as the two red points in the inset). In these figures the lower branch corresponds to the phase directly given by Eq. (11), while the upper one is obtained after unwrapping the

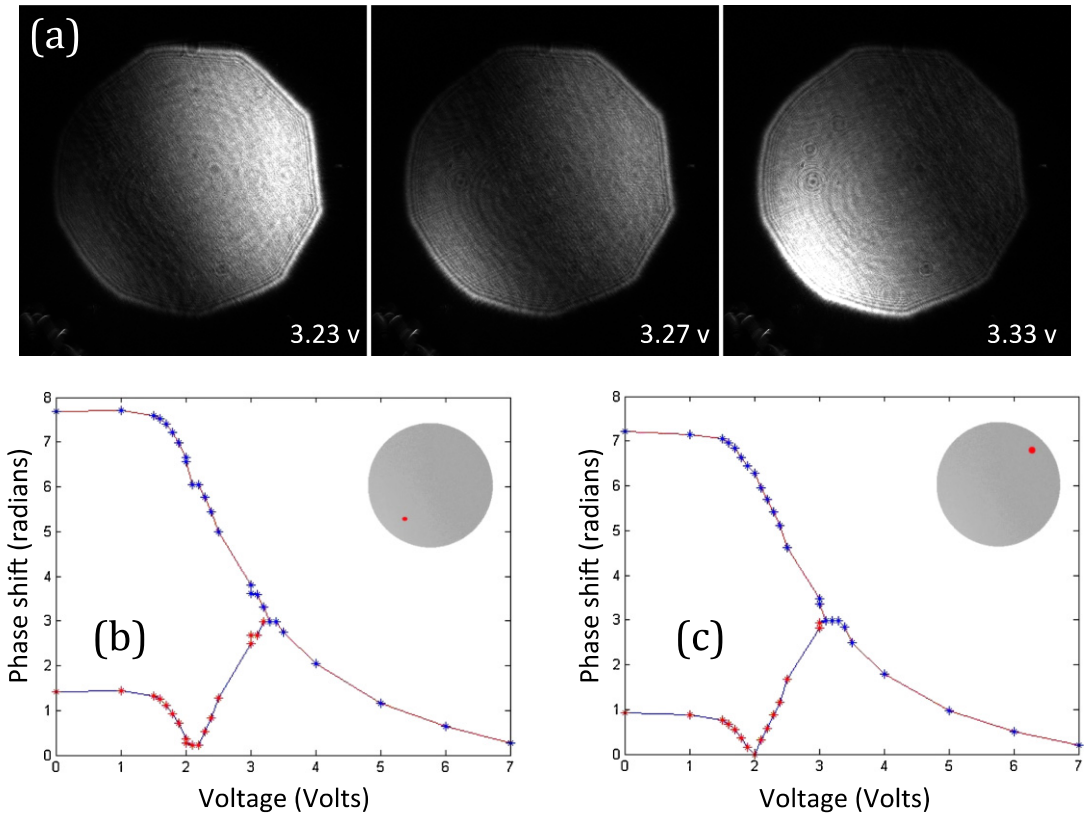

Fig. 7. (Color online) (a) Images of the LCR with parallel polarizers and monochromatic illumination of 633 nm for different applied voltages; (b, c) Retardance (in rad) versus voltage for 633 nm at two different points of the LCR (their location on the LCR surface is indicated by the red points in the inset).

function. From these results one can conclude that a maximum retardance variation of more than 0.5 rad (approximately 30°) occurs for $\lambda = 633$ nm from the top-right area to the bottom-left area of the LCR. This value corresponds to the situation at zero voltage, when the retardance is maximum. When a voltage is applied to the device, the retardance values are reduced according to the data in Figs. 7(a) and 7(b), but always showing a spatial variation. This non-uniformity of the device must be taken into account, especially when operating at low voltages.

5. Conclusions

In summary, we have presented a simple technique to spectrally characterize the retardance of a variable LCR, and provide a full description on the basis of few parameters of a simplified model of the device.

Spectral measurements of the light transmitted by the polarizer–LCR–analyzer system are considered. Measurements in absence of driving voltage are used to derive the retardance dependence according to the well-established first order Cauchy type dispersion of the refractive indices. Two numerical Cauchy dispersion parameters, A_0 and B_0, are enough to provide an accurate description. Then, we demonstrated that, if the Cauchy dispersion relation is well suited in the off state of the device, when maximum retardance is obtained, the voltage dependant effective retardance also follows this type of dispersion. Their evolution is described with a single voltage transfer function $g(V)$, valid for the complete wavelength range.

The proposed procedure provides an accurate evaluation of the retardance versus wavelength and versus voltage in a single set of experiments. The retardance is fully characterized with just the two numerical parameters, A_0 and B_0, and the transfer function $g(V)$. From these data, the retardance $\phi_V(\lambda)$ can be fully retrieved for any applied voltage and any wavelength within the selected range. In addition, these are absolute measurements of the retardance, as opposed to most of the methods that provide the relative (modulo 2π) retardance. Note that the Cauchy fitting procedure is advantageous since it directly provides the complete retardance evolution, without requiring any phase unwrapping technique.

Finally, we have reported a non-negligible spatial variation in retardance. We developed a simplified imaging polarimeter in order to evaluate the retardance at each point of the LCR. The developed procedure leads to a precise characterization of this type of modulator devices, which is a requisite for their proper use in other advanced optical measurement systems, such as polarimeters or programmable optical transmission filters.

This procedure can be useful for users of commercial LCR devices, which usually do not have information about internal details such as refractive indices and its wavelength variation. Note that it can be applied to modern parallel

aligned liquid crystal on silicon (LCoS) devices. The method does not require advanced equipment, expect for a spectrometer. This kind of precise characterization might be very relevant prior to the use of LCR in polarimetric or interferometric systems.

Acknowledgements

This work has been financed by grant Fondecyt No. 1110937 and Center for Optics and Photonics (CEFOP) FB0824/2008. MMSL and IM acknowledge financial support from the Spanish Ministerio de Economía y Competitividad and fondos FEDER, through the project FIS2012-39158-C02-02.

References

1) Web [http://www.meadowlark.com/, http://www.thorlabs.com/, http://www.arcoptix.com/].
2) L.-H. Shyu, C.-L. Chen, and D.-C. Su: Appl. Opt. **32** (1993) 4228.
3) W.-K. Kuo, J.-Y. Kuo, and C.-Y. Huang: Appl. Opt. **46** (2007) 3144.
4) C.-H. Hsieh, C.-C. Tsai, H.-C. Wei, L.-P. Yu, J.-S. Wu, and C. Chou: Appl. Opt. **46** (2007) 5944.
5) Y.-T. Jeng and Y.-L. Lo: Appl. Opt. **45** (2006) 1134.
6) S.-T. Wu: Phys. Rev. A **33** (1986) 1270.
7) A. Hollstein and T. Ruhtz: Opt. Lett. **34** (2009) 2599.
8) P. Velasquez, M. M. Sánchez-López, I. Moreno, D. Puerto, and F. Mateos: Am. J. Phys. **73** (2005) 357.
9) M. Emam-Ismail: Opt. Laser Technol. **41** (2009) 615.
10) S.-T. Wu, U. Efron, and L. D. Hess: Appl. Opt. **23** (1984) 3911.
11) N. Fukuchi, Y. Biqing, Y. Igasaki, N. Yoshida, Y. Kobayashi, and T. Hara: Opt. Rev. **12** (2005) 372.
12) H. Mada and S. Kobayashi: Mol. Cryst. Liq. Cryst. **33** (1976) 47.
13) T.-L. Kelly and J. Munch: Opt. Commun. **156** (1998) 252.
14) J. S. Gwag, S. H. Lee, K.-Y. Han, J. C. Kim, and T.-H. Yoon: Jpn. J. Appl. Phys. **41** (2002) L79.
15) S. H. Lee, W. S. Park, G.-D. Lee, K.-Y. Han, T.-H. Yoon, and J. C. Kim: Jpn. J. Appl. Phys. **41** (2002) 379.
16) I. Moreno, A. M. Cutillas, M. M. Sánchez-López, P. Velásquez, and F. Mateos: Opt. Commun. **281** (2008) 5520.
17) J. Li, C.-H. Wen, S. Gauza, R. Lu, and S.-T. Wu: J. Disp. Technol. **1** (2005) 51.
18) A. Marino, E. Santamato, N. Bennis, X. Quintana, J. M. Otón, V. Tkachenko, and G. Abbate: Appl. Phys. Lett. **94** (2009) 013508.
19) B. E. A. Saleh and K. Lu: Opt. Eng. **29** (1990) 240.
20) R. A. Herke, M. H. Anderson, and T. G. Baur: Proc. SPIE **3800** (1999) 45.
21) J. Vargas, N. Uribe-Patarroyo, J. Antonio Quiroga, A. Alvarez-Herrero, and T. Belenguer: Appl. Opt. **49** (2010) 568.
22) J. Otón, P. Ambs, M. S. Millán, and E. Pérez-Cabré: Appl. Opt. **46** (2007) 5667.
23) P. Beatriz Garcia-Allende and O. M. Conde Portilla: Opt. Pura Apl. **45** (2012) 345 [in Spanish].